Kashf Journal of Multidisciplinary Research
Vol:03 - Issue02(2026)
P-ISSN: 3007-1992 E-ISSN: 3007-200X
https://kjmr.com.pk

EXPERIMENTAL INVESTIGATION OF TITANIUM COATING FOR CORROSION RESISTANCE ON STAINLESS STEEL GRADE ASTM 304L AND 316L FOR MEDICAL APPLICATION

Syed Nasir Mehdi Gardezi[1], Asad Raza Gardezi[2], *Ali Nawaz Sanjrani[3], Muhammad Punhal Sahto[4], Muhammad Hassan[5], Arfa[6], Ali Raza[7]

[1, 4, 5, 6, 7]NFC Institute of Engineering and Technology, Multan, Pakistan.
[2]Bahauddin Zakariya University, Multan, Pakistan.
[3]Mehran University of Engineering and Technology, SZAB Campus Khairpur Mir's, Pakistan.

Corresponding Author:(nawaz.sanjrani2019@gmail.com; nasirgardezi@nfciet.edu.pk)
DOI:(*https://doi.org/10.71146/kjmr831*)

Article Info

Abstract

This research study investigates the surface enhancement of austenitic stainless steels ASTM 304L and 316L for biomedical implant applications through a titanium dioxide (TiO_2) thin film deposited by physical vapor deposition (PVD). This study aims to determine whether a TiO_2 coating can improve corrosion resistance in physiologically relevant environments while maintaining or enhancing key mechanical characteristics required for load-bearing medical components. Uncoated and coated specimens of both grades were evaluated using electrochemical corrosion testing, mechanical testing (hardness and compressive strength), and microstructural/chemical characterization by scanning electron microscopy (SEM) coupled with energy-dispersive X-ray spectroscopy (EDS). The TiO_2-coated samples exhibited a clear improvement in corrosion behavior compared with the uncoated substrates, indicating a more protective surface and reduced susceptibility to degradation. Mechanical results showed a modest increase in surface hardness and a slight improvement in compressive performance after coating, suggesting that the deposited layer contributed to better surface integrity without compromising bulk response. Among the investigated materials, TiO_2-coated 316L demonstrated superior overall performance relative to TiO_2-coated 304L, consistent with the higher intrinsic corrosion resistance of 316L and the effectiveness of the coating–substrate combination. SEM examination revealed a uniform, dense coating morphology with no visible cracking or delamination, while EDS confirmed the presence and continuity of the TiO_2 layer. These findings support PVD-deposited TiO_2 as a practical route to improve the corrosion resistance and surface performance of stainless-steel alloys intended for biomedical implant service.

Keywords: *Titanium dioxide (TiO_2); Physical Vapor Deposition (PVD); Stainless Steel Grade 304l and 316l; Biomedical.*

1 Introduction

Corrosion resistance and biocompatibility are critical factors in the design and fabrication of biomedical implants and high-performance materials. Stainless steels, particularly AISI 316L, and titanium-based alloys are widely used due to their favorable mechanical properties, chemical stability, and biocompatibility. However, these materials are susceptible to corrosion and wear in physiological environments, requiring surface modification through coatings and thin films. Nano coatings of Alumina, Titania, and multilayer combinations have been deposited on stainless steel via Atomic Layer Deposition (ALD) at 250°C, with morphology and elemental composition characterized using SEM and EDX [1,16]. Corrosion studies in simulated body fluid (SBF) at 37°C, including open-circuit potential, Tafel extrapolation, and cyclic polarization, demonstrated that multilayer coatings provide superior corrosion resistance compared to single-layer films, with Alumina exhibiting higher resistance than Titania [1,5,19]. Biocompatibility and bioactivity tests using non- pathogenic E. coli confirmed the non-toxic nature of these coatings, indicating their suitability for biomedical applications [1,16,19].

Titanium and its alloys, including Ti6Al4V and NiTi shape memory alloys, have also been extensively studied due to their excellent mechanical strength, corrosion resistance, and biocompatibility [8–10,17,21,30,31]. Coatings such as Ti, TiO_2, TiN, N-TiO_2, and TiN/ZrN have been fabricated via plasma surface alloying, PVD, anodization, and atmospheric plasma spraying, enhancing polarization resistance, reducing corrosion current density, and improving wear and tribological corrosion behavior [2– 7,10,12,28]. Incorporating elements such as Zr, as well as bio-ceramic coatings like hydroxyapatite (HA) composites with TiO_2 or ZrO_2, further improves electrochemical stability, surface hardness, and corrosion resistance in simulated body fluids and chloride-containing solutions [5,11,15,16,19,22,27,30]. Advanced hybrid coatings, including Ti/TiO_2-N, TiN/ZrN, and Ag/Co_3O_4/TiO_2 nanocomposites, exhibit enhanced charge transfer resistance, reduced corrosion rates, and better structural integrity due to dense columnar microstructures and synergistic effects between coating materials [7,16,19,28]. Microstructural evolution and mechanical properties of substrate materials, including as-cast and wrought stainless steel 316L and 304L, significantly affect coating performance. Factors such as recrystallization behavior, grain orientation, and delta ferrite content influence coating adhesion, hardness, and corrosion resistance [4]. Additionally, deposition techniques, coating thickness, surface morphology, and post-treatment processes such as heat treatment, anodization, or vacuum sintering play a critical role in electrochemical and tribological performance [5,15,30]. Functionally graded materials (FGMs) and nanocomposite coatings have demonstrated that optimizing composition, microstructure, and deposition parameters substantially improves corrosion resistance, mechanical strength, and biocompatibility, making these surfaces suitable for long-term implant applications and demanding industrial uses [6,19,22,28,31]. Overall, literature shows that the choice of coating material, deposition method, and post-processing treatment are essential for achieving durable, corrosion-resistant, and biocompatible stainless steel and titanium- based implants.

This study aims at exploiting experimental evidence on corrosion resistance and biocompatibility improvement of stainless-steel grade 304L and 316L in medical applications due to titanium-based coating. The work is concentrated in depositing Ti, TiO2, TiN, hybrid and characterization of the surface morphology, microstructure and elemental composition using SEM, EDX, XRD, and AFM respectively. The corrosion performance of the coated and uncoated substrates will also be determined in simulated body fluids, as well as in chloride-containing aqueous solutions using open-circuit potential, Tafel extrapolation, cyclic polarization and electrochemical impedance spectroscopy (EIS). Besides, the effects of coating composition, thickness, and multilayers as well as substrate microstructure on adhesion, mechanical properties and electrochemical performance will be evaluated. The biocompatibility and biological performance/-bioactivity of the coating will also be investigated in terms of bacteria culture efficiency, and through in vitro test immersion SBF, with the final aim to determine the most

appropriate titanium coating configuration to achieve better resistance toward corrosion and to perform in biological applications in the long-term.

2 Experimental methods

2.1 Theoretical Considerations

The corrosion behavior of stainless steels in chloride-containing and physiological environments is primarily governed by the stability of the native passive film, which may locally break down in the presence of chloride ions and initiate pitting. To systematically quantify the effect of a PVD-deposited TiO_2 barrier on this behavior, the study followed the methodological framework shown in Figure 1, beginning with substrate selection (SS304L and SS316L), coupon preparation (cutting and hole drilling for consistent fixturing), and controlled surface finishing, cleaning, and nitrogen drying to establish a reproducible baseline condition.

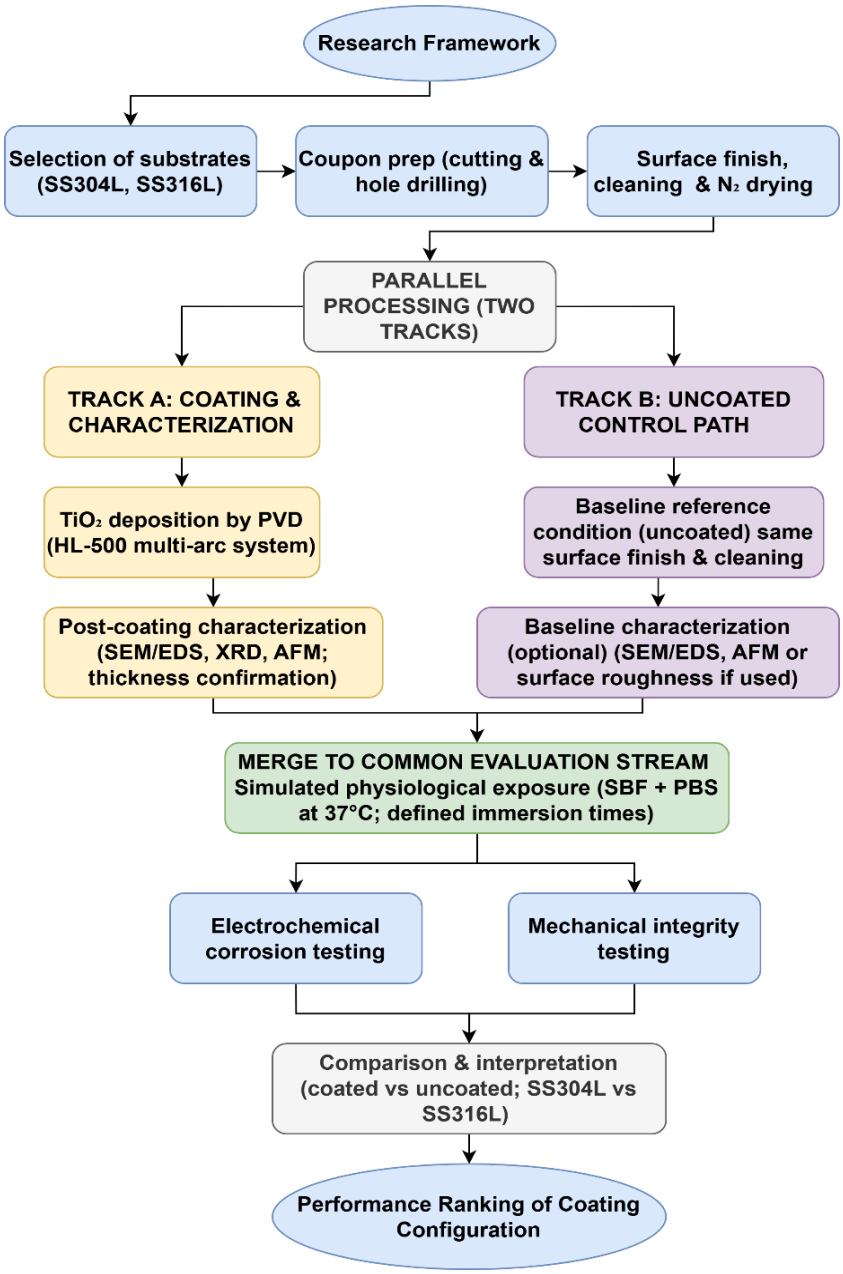

Figure 1 Methodological flowchart for TiO_2 coating fabrication and performance assessment on SS304L and SS316L.

The workflow then bifurcated into two parallel tracks to isolate the coating contribution: Track A involved TiO_2 deposition using the HL-500 multi-arc PVD system followed by post-coating characterization (SEM/EDS, XRD, and AFM with thickness confirmation), whereas Track B retained uncoated specimens prepared under identical surface conditions as reference controls. Both tracks subsequently converged into a common evaluation stream comprising exposure in simulated physiological media (SBF and PBS at 37 °C for defined immersion durations), electrochemical corrosion testing, and mechanical integrity assessment, after which results were compared between coated and uncoated states and between SS304L and SS316L to establish performance ranking. TiO_2 is expected to enhance corrosion resistance by providing a chemically stable, adherent barrier that limits aggressive ion transport and suppresses interfacial charge transfer; correspondingly, improved protection is anticipated to manifest in electrochemical impedance spectroscopy as increased polarization/charge-transfer resistance and reduced interfacial capacitance due to decreased electrochemically active area and improved film integrity

2.2 Stainless Steel Substrates

Two austenitic stainless-steel grades, SS316L and SS304L, were selected as substrates to represent widely used biomedical stainless steels with different alloying characteristics. SS316L was chosen due to its established use in biomedical devices and implants, where its mechanical strength and corrosion resistance are enhanced by molybdenum addition and its low-carbon composition supports improved resistance to sensitization. SS304L was used as a comparative substrate because its low carbon content supports corrosion resistance relative to standard 304, while its different alloy chemistry provides a meaningful basis to examine how TiO_2 coating modifies corrosion response and interfacial electrochemical behavior under chloride and physiological conditions.

2.3 Materials and Sample Preparation

2.3.1 Substrate Preparation Cutting and Fixturing

Stainless-steel plates were first sectioned into coupons using a precision cutting approach to ensure dimensional consistency and to minimize thermal distortion of the substrate. The initial stock material was cut into 10 × 10 cm sections and subsequently machined into test coupons, after which a mounting hole was introduced using a drilling machine to facilitate safe handling and repeatable fixturing during PVD coating and subsequent experimental measurements. Following machining, all specimens were subjected to a standardized surface preparation protocol to obtain a reproducible surface condition prior to deposition. Specifically, the coupon surfaces were progressively ground using silicon carbide (SiC) abrasive papers up to 1200 grit to remove cutting-induced irregularities and to achieve a uniform surface finish. Final polishing was then carried out using alumina slurry to obtain a mirror-like surface, which is critical for reducing surface defects that may serve as preferential sites for coating discontinuities and localized corrosion initiation. After polishing, the specimens were ultrasonically cleaned in ethanol and acetone for 15 min to remove residual polishing media, oils, and other surface contaminants, and then dried under nitrogen to limit oxidation prior to coating. As shown in Figure 2, the SS304L coupons produced by the wire-cutting/precision cutting process exhibit well-defined geometry and smooth, burr-free edges, which are essential for repeatable coating deposition and electrochemical testing. The controlled coupon geometry and carefully prepared surface condition not only support uniform TiO_2 film growth during PVD but also enhance the reliability of corrosion measurements by minimizing variability associated with edge effects and surface roughness differences among specimens.

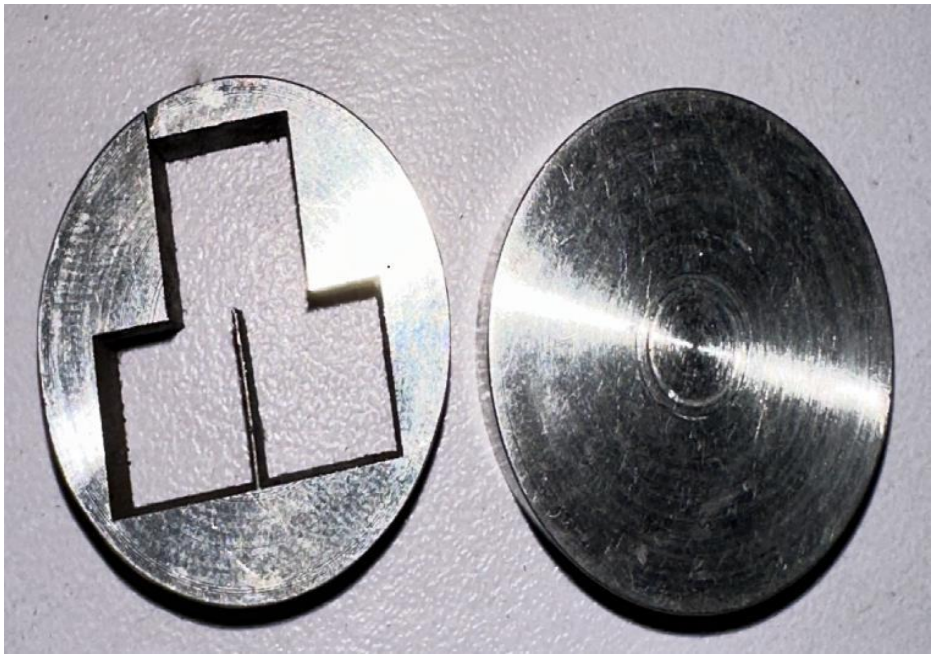

Figure 2 SS304L Samples cut by wire cutting method

Similarly, as shown in Figure 3, representative SS316L coupons were fabricated using a wire-cutting/precision cutting route to obtain specimens with consistent dimensions and controlled edge quality for subsequent coating and testing. The figure presents two conditions of the SS316L specimen: the coupon on the left shows the immediate post-cut state, where machining marks and localized surface irregularities can still be observed, while the coupon on the right illustrates the final prepared surface after grinding and polishing, exhibiting a more uniform, mirror-like finish. Establishing this reproducible surface condition is essential for achieving homogeneous TiO_2 film deposition by PVD and for minimizing variability in electrochemical measurements, since surface defects and roughness can promote localized corrosion initiation and affect impedance response.

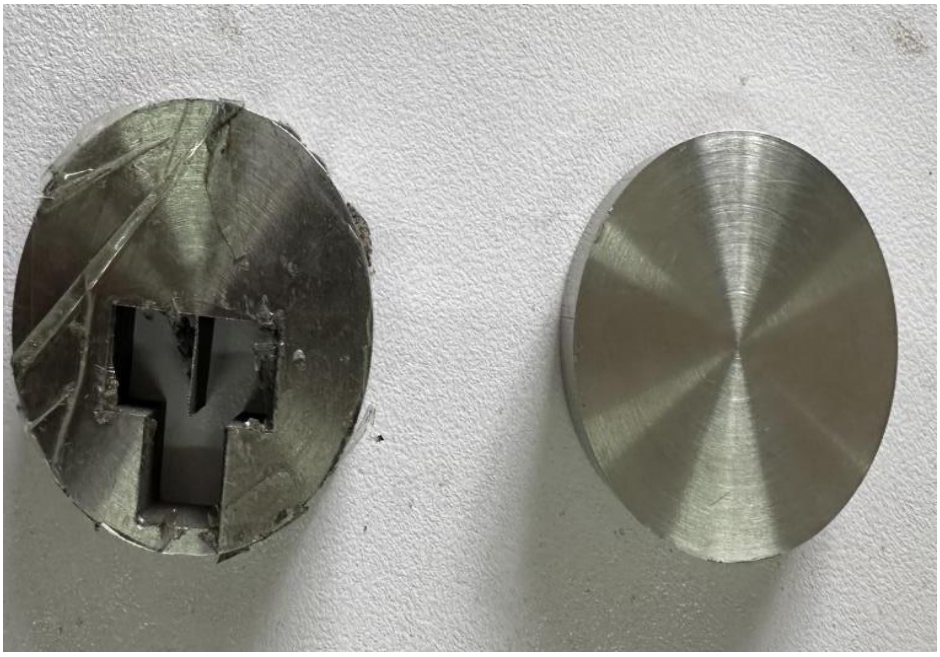

Figure 3 SS316L Samples cut by wire cutting method

A drilling operation was performed to introduce a standardized mounting hole in each stainless-steel coupon to enable safe handling and reliable fixturing during the PVD coating process and subsequent testing. As shown in Figure 4, the specimens were securely clamped on the drilling table and machined under controlled conditions to ensure a consistent hole geometry across all samples.

Figure 4 Drilling process on samples for coating

This mounting feature facilitated repeatable positioning of the coupons within the PVD chamber, thereby maintaining stable orientation during deposition and supporting uniform coating exposure. In addition, the use of a uniform mounting approach reduced specimen-to-specimen variability during later characterization and electrochemical corrosion measurements by ensuring consistent handling and minimizing the risk of surface damage.

2.4 Titanium Dioxide Coating via PVD

Titanium dioxide (TiO_2) coatings were deposited on the mirror-polished SS304L and SS316L coupons using a Physical Vapor Deposition (PVD) process performed with an HL-500 multi-arc vacuum coating system. As shown in Figure 5, the deposition was carried out using titanium as the cathodic target material in a reactive, oxygen-rich atmosphere to promote in situ formation of TiO_2 during arc evaporation. The substrate temperature was controlled within the range of 250–320 °C to enhance coating adhesion and support stable film growth, while the coating thickness was regulated to approximately 1.2 µm through deposition time and process settings. These operating conditions were selected to achieve a dense and continuous ceramic barrier layer with minimal macroscopic defects, since discontinuities, pinholes, or thickness non-uniformity can significantly affect localized corrosion initiation in chloride- and body-fluid environments. Following deposition, all specimens were handled using the mounting arrangement described earlier to maintain consistent positioning during coating and to reduce variability associated with fixturing and edge effects

Under the controlled environment as shown in Figure 5, the HL-500 multi-arc vacuum coating machine comprises a sealed deposition chamber coupled with dedicated power and control cabinets that regulate key process variables such as arc current, chamber pressure, gas flow, and substrate heating. The vacuum chamber (left) provides a controlled low-pressure environment that minimizes contamination and enables stable plasma generation, while

the control units (right) allow real-time monitoring and repeatable adjustment of deposition conditions. This level of control is particularly important for biomedical-grade coatings because the corrosion performance of TiO_2 films is highly sensitive to process stability; fluctuations in oxygen partial pressure, substrate temperature, or arc behavior can alter coating density and defect population, which in turn influences barrier integrity and electrochemical response in simulated physiological media.

Figure 5 HL-500 multi arc vacuum coating machine

For coating material first cleaned by mirror polishing by alumina slurry polish. After that Titanium dioxide coating applied by physical vapor deposition method on these samples. The results for Titanium dioxide coating on SS304l and SS316L are given in Figure 6.

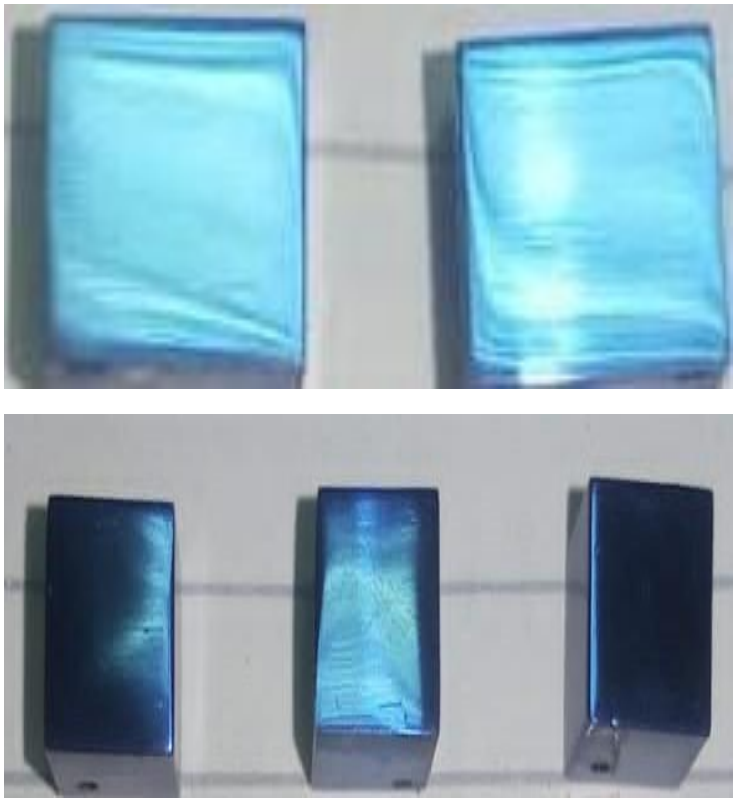

Figure 6 Titanium dioxide coating on SS304l

After deposition, the coated specimens were examined visually as an initial quality-control step prior to detailed microstructural and electrochemical characterization. Representative coated samples are presented in Figure 6, where the uniform surface appearance and consistent coloration across the coupons provide qualitative confirmation of continuous coating coverage and stable deposition conditions. Such visual uniformity is practically important because patchy deposition, shadowing, or surface discoloration gradients often indicate thickness variations or localized defects that can later serve as preferential sites for coating breakdown under electrochemical exposure. The coated specimens shown in Figure 6 were subsequently advanced to post-coating characterization (SEM/EDS, XRD, and AFM) and corrosion testing in simulated physiological media, enabling direct correlation between coating formation quality, microstructural features, and the measured electrochemical performance.

2.5 Simulated Physiological Environment

The coated and un-coated samples were submerged in the following to replicate them in vivo environment:

- SBF (Simulated Body Fluid)
- PBS (Phosphate Buffered Saline)

As per design procedure and to reproduce relevant physiological conditions, coated and uncoated specimens were exposed to simulated body fluids using SBF and phosphate-buffered saline (PBS). Both solutions were prepared according to standard formulations and maintained at 37 °C to represent human-body temperature. The immersion duration was varied to evaluate both short-term and longer-term electrochemical stability, with the intention of observing whether the coating maintains barrier performance and whether the surface condition changes over time in physiologically relevant electrolytes.

2.6 Corrosion Testing

The corrosion resistance of coated and uncoated stainless- steel samples was investigated using electrochemical impedance spectroscopy. Potentiostat Reference - 3000 was used for Potentiodynamic characterization with three electrode systems (Figure 6).

The following were part of the experimental setup:

- Electrochemical cell: arrangement of three electrodes
- Stainless steel sample as the working electrode
- Ag/AgCl is the reference electrode.
- Platinum is the counter electrode

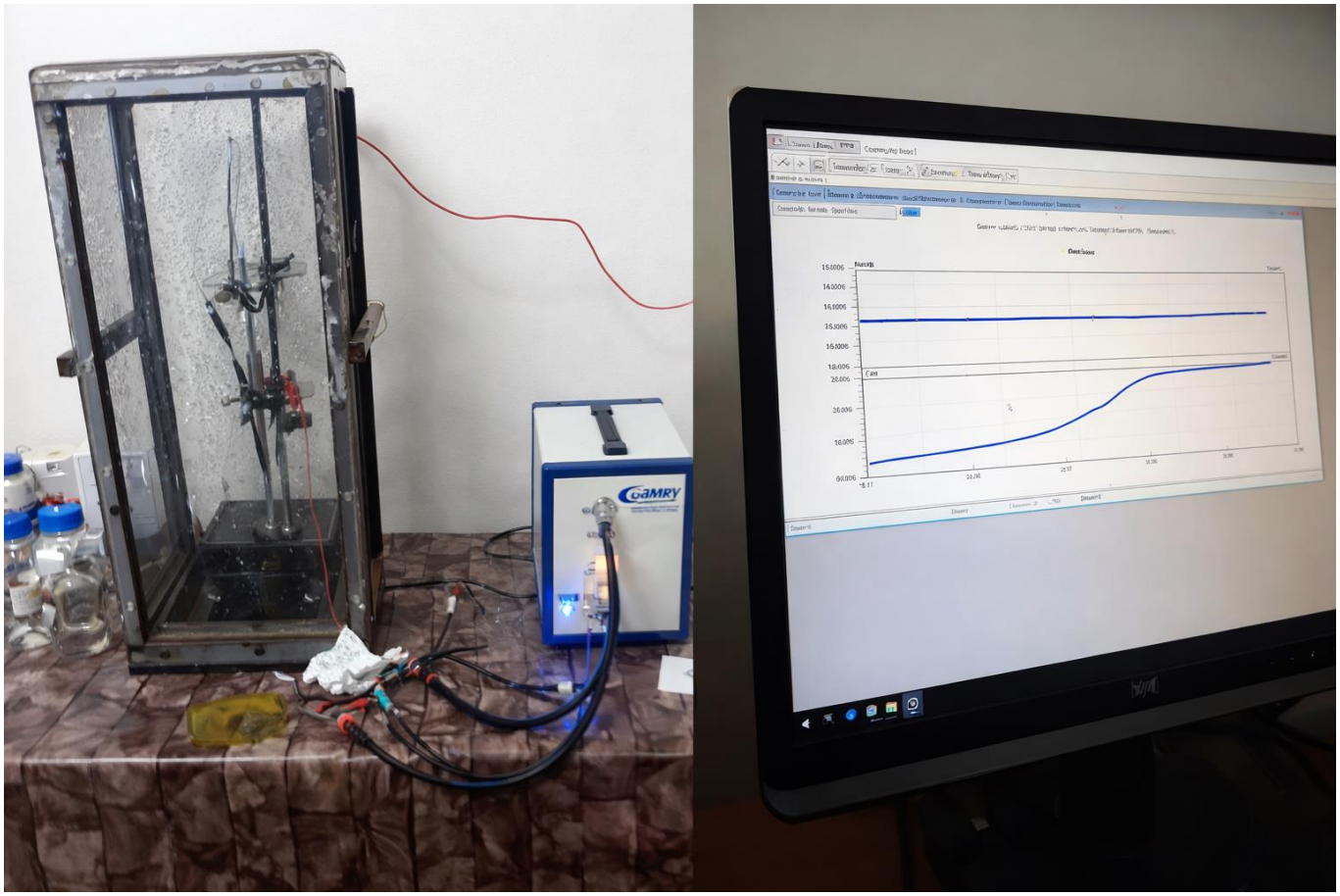

Figure 7 Potentiostat Reference-3000 setup for Potentiodynamic characterization of as -synthesized electrodes

Electrochemical corrosion performance was evaluated using a three-electrode configuration connected to a potentiostat as mentioned above in section 2.6. In this arrangement, the stainless-steel specimen served as the working electrode, an Ag/AgCl electrode was used as the reference electrode, and platinum was employed as the counter electrode. Prior to impedance testing, the working electrode was stabilized at open-circuit conditions to allow the interface to reach a steady electrochemical state in the test solution. Electrochemical impedance spectroscopy measurements were then performed over a frequency range of 10^5 to 10^{-2} Hz. The resulting impedance spectra were interpreted using equivalent circuit modeling to extract interfacial parameters, including charge transfer resistance and double-layer capacitance (or constant phase element parameters), which were used as quantitative indicators of coating integrity and corrosion resistance. The corrosion behavior of coated specimens was compared directly against uncoated SS304L and SS316L under the same electrolyte and temperature conditions to isolate the effect of TiO_2 coating.

2.7 Mechanical Integrity Testing

Mechanical integrity was evaluated to determine whether TiO_2 deposition affects the near-surface mechanical response of the substrate coating system and to ensure that corrosion improvement is not achieved at the expense of mechanical reliability. Microhardness measurements were carried out using a Vickers hardness tester under a fixed load and dwell time to enable consistent comparison between coated and uncoated conditions. In addition, compressive testing was performed using a universal testing machine at a controlled strain rate to verify that the coating process (including the thermal exposure during deposition) does not adversely influence the bulk mechanical behavior of SS304L and SS316L. Given that the TiO_2 film thickness is on the order of micrometers, hardness is expected to be more sensitive to surface modification than compressive strength;

therefore, the compressive response is interpreted primarily as a substrate/process verification metric, while hardness trends are used to reflect coating-associated surface strengthening or changes in near-surface deformation behavior. The mechanical results were then discussed alongside electrochemical outcomes to establish whether enhanced corrosion resistance is achieved without compromising overall mechanical performance.

2.8 Microstructural Investigation

Microstructural characterization was conducted to verify the formation quality of the TiO_2 coatings and to establish structure property relationships between surface condition, coating integrity, and the measured electrochemical performance in simulated physiological media. In this study, scanning electron microscopy (SEM), complemented by energy-dispersive X-ray spectroscopy (EDS), was employed as the primary technique to evaluate both the morphological features and elemental distribution of coated and uncoated SS304L and SS316L specimens. The SEM platform used for this work is shown in Figure 8, which illustrates the instrumentation employed for high-resolution imaging and integrated compositional analysis.

Figure 8 Pictorial view of scanning electron microscope

SEM examination was performed on the as-prepared substrates and on the TiO_2-coated surfaces to assess surface topography and coating continuity at multiple magnifications. Particular attention was given to identifying coating-related features such as microcracks, discontinuities, porosity, and droplet-like defects that may arise in arc-based PVD coatings, as these features can serve as preferential pathways for electrolyte ingress and localized corrosion initiation. The comparison between coated and uncoated specimens enabled evaluation of how the coating process altered the surface morphology relative to the baseline polished condition, including any changes in surface texture and the appearance of microstructural contrast. In addition, SEM imaging was used to judge the homogeneity of coating coverage across the coupon surface, including regions near edges and mounting features, where thickness gradients or shadowing effects may occur during deposition. These morphological observations were subsequently used to support interpretation of electrochemical trends, since a more continuous and defect-minimized surface is expected to yield higher barrier performance and improved impedance response. EDS was employed to confirm the elemental composition of the surfaces and to verify successful TiO_2 formation on both stainless-steel grades. Using the SEM/EDS system shown in Figure 8, EDS spectra and elemental maps were acquired to detect the presence and spatial distribution of titanium and oxygen on coated specimens and to compare these results with uncoated controls. This step was essential to ensure that differences in corrosion behavior were attributable to TiO_2 coating formation rather than to surface contamination or incomplete film coverage. For coated samples, the expected outcome was surface enrichment in Ti and O accompanied by a

reduced apparent contribution from substrate elements such as Fe, Cr, and Ni (and Mo in SS316L), which would indicate a continuous coating layer. Conversely, strong substrate signals together with weak Ti/O response would suggest partial coverage or coating discontinuity, conditions that typically correlate with reduced protective performance. EDS mapping further provided insight into localized compositional variations that may be associated with deposition non-uniformity, coating defects, or regions susceptible to accelerated degradation. Overall, SEM/EDS characterization which was performed using the instrument shown in Figure 8 also provided direct evidence of coating integrity and elemental composition, thereby forming a microstructural basis for interpreting the corrosion and mechanical results. The integration of surface morphology assessment with elemental verification enabled a consistent evaluation of how TiO_2 deposition quality influences electrochemical parameters and long-term stability in simulated physiological environments.

3 Result and Discussion

3.1 Corrosion Resistance Analysis

Electrochemical Impedance Spectroscopy (EIS) results reveal significant improvement in the corrosion resistance of TiO_2-coated stainless-steel samples as compared to their uncoated counterparts. Titanium dioxide coatings have been shown to be useful in improving the corrosion resistance of metallic implants using electrochemical impedance spectroscopy experiments. Ion-beam-assisted sputtering of TiO_2 films onto stainless-steel substrates resulted in lower passive current density and higher electrical resistance than naturally occurring oxide coatings. Long-term stability of titanium's passive oxide coating is demonstrated in phosphate-buffered solutions; however, the addition of H_2O_2 can thicken the porous outer layer and reduce corrosion resistance. Nyquist plots Figure 9 showed larger semicircle diameters for coated samples, indicating higher charge transfer resistance (Rct). Among the samples, SS-316L with TiO_2 coating exhibited the highest Rct, followed by coated SS-304L. Uncoated samples displayed smaller arcs, suggesting lower corrosion resistance.

Table 1: Charge Transfer Resistance ($R_{ct}$from EIS) and current densities

Sample	R_{ct} (kΩ·cm²)	i_{corr} (µA/cm²)	Literature Range
SS-304L (Uncoated)	2.5	20.8	5-50 µA/cm²
SS-304L (Coated)	8.3	6.27	1-10 µA/cm²
SS-316L (Uncoated)	4.1	12.68	5-30 µA/cm²
SS-316L (Coated)	12.7	4.09	1-5 µA/cm²

This enhancement is attributed to the passive barrier layer of TiO_2, which prevents the diffusion of aggressive ions in simulated body fluid. This finding aligns with previous reports on titanium oxide's ability to form a chemically stable and biocompatible barrier [32]. The electrochemical impedance spectroscopy (EIS) results demonstrated a significant enhancement in the corrosion resistance of the TiO_2-coated samples compared to the uncoated ones. The charge transfer resistance (Rct) values were considerably higher for the coated samples. Specifically, the $Rct$of SS-304L increased from 2.5 kΩ·cm² (uncoated) to 8.3 kΩ·cm² (coated), while SS-316L showed an increase from 4.1 kΩ·cm² to 12.7 kΩ·cm² (Table 1).

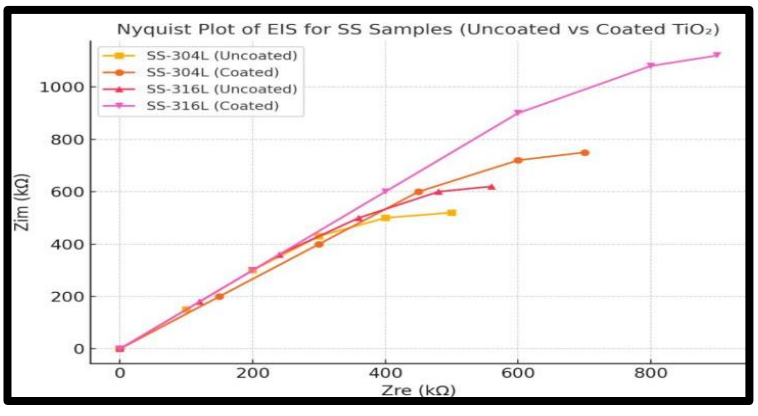

Figure 9 EIS Nyquist Plot for SS 304L and 316L samples (Uncoated & Coated TiO2)

This improvement is attributed to the formation of a stable and adherent TiO_2 film that acts as a physical barrier, hindering the transport of corrosive species from the simulated body fluid (SBF) to the metal substrate [33]. These findings are consistent with the results reported by Ganesan and Rajeswari [34], who noted improved passivation behavior and decreased corrosion rates with TiO_2 coatings in biomedical environments.

The ranking of corrosion resistance based on semicircle diameters is as follows and illustrated in Figure 9:

SS-316L (Coated) > SS-304L (Coated) > SS-316L

(Uncoated) > SS-304L (Uncoated)

This trend underscores the dual benefits of selecting high- performance base alloys (like SS-316L) and applying functional coatings (like TiO_2). These findings are aligned with previous studies that confirm the ability of TiO_2 coatings to significantly reduce corrosion currents and increase charge transfer resistance [35-36].

The TiO_2 layer deposited through PVD offers a dense, uniform, and adherent film that prevents the ingress of chloride ions a primary cause of corrosion in biological environments. The enhanced impedance also reflects the minimized electrochemical activity at the metal– electrolyte interface, which is crucial for long-term implant safety [37]. Furthermore, TiO_2 has been shown to support bio integration and tissue compatibility, further justifying its use in biomedical device applications [38].

3.2 Mechanical Properties

The mechanical testing results indicate a slight increase in surface hardness due to TiO_2 coating. Vickers hardness values increased by approximately 8–12% for coated samples. SS-316L demonstrated higher hardness than SS-304L in both coated and uncoated states, consistent with its alloy composition.

The Vickers hardness values also showed (Table 2) a noticeable increase after coating. SS-304L had a hardness of 185 HV, which increased to 202 HV after TiO_2 deposition. Similarly, SS-316L increased from 210 HV to 228 HV. The enhancement in surface hardness can be linked to the intrinsic hardness of TiO_2 and its uniform deposition across the substrate [39].

This slight improvement in surface hardness without compromising ductility or bulk mechanical properties indicates that the coating does not adversely affect the load-bearing capacity of the implants, which is a crucial requirement for biomedical applications [40].

Table 2: Vickers' Hardness Values

Sample	Hardness (HV)
SS-304L (Uncoated)	185
SS-304L (Coated)	202
SS-316L (Uncoated)	210
SS-316L (Coated)	228

Table 3: Compressive strength value with relative increase due to coating

Sample	Compressive strength	Relative increase due to coating (%)
SS-304L (Uncoated)	410	-
SS-304L (TiO_2-Coated)	436	+6.3%
SS-316 (Uncoated)	445	-
SS-316L (TiO_2-Coated)	475	+6.7%

Compressive strength testing (Table 3) showed negligible variation in ultimate compressive strength between coated and uncoated samples, suggesting that the TiO_2 layer does not compromise the structural integrity. The mechanical behavior remained stable even under elevated temperature testing (up to 100 °C), indicating good thermal stability, which is crucial for in-vivo conditions [41]. TiO_2-coated samples exhibited a modest improvement in compressive strength compared to their uncoated counterparts. The increase 7% can be attributed to the confinement effect of the coating, which reduces micro crack initiation at the surface and distributes applied load more evenly [35]. SS-316L consistently showed superior compressive strength over SS-304L, owing to its enhanced alloying with molybdenum and higher austenitic stability. These findings suggest that TiO_2 coatings do not compromise mechanical performance and may even enhance it, reinforcing their suitability for load-bearing biomedical implants [38].

3.3 Microstructural Analysis

SEM micrographs showed uniform deposition of TiO_2 on the stainless-steel surfaces 304L and 316L with no visible cracks or delamination (Figure 9 and 10). The coated surface exhibited a fine grain structure with evenly distributed particles, enhancing surface area and providing better protection against corrosion. The micrograph clearly depicts that the coated film is free from defects and microcracks and has excellent homogeneity and large surface area.

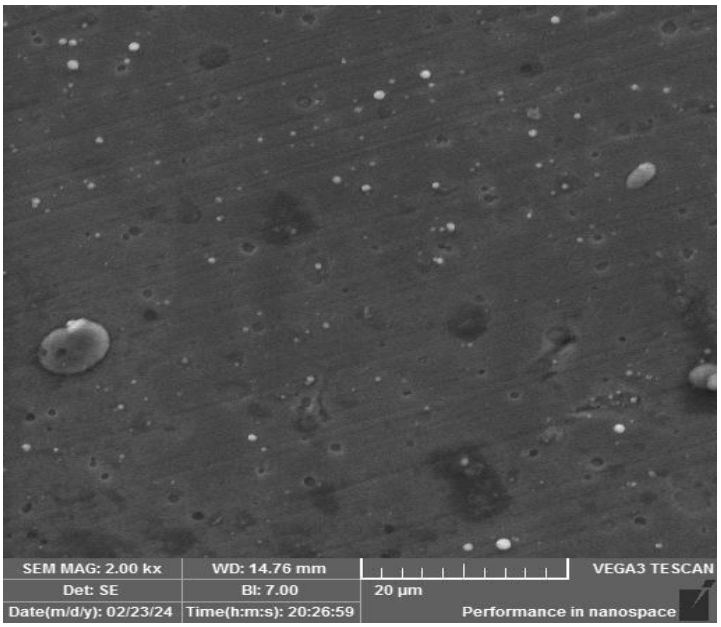

Figure 10 Uncoated SS304l SEM results

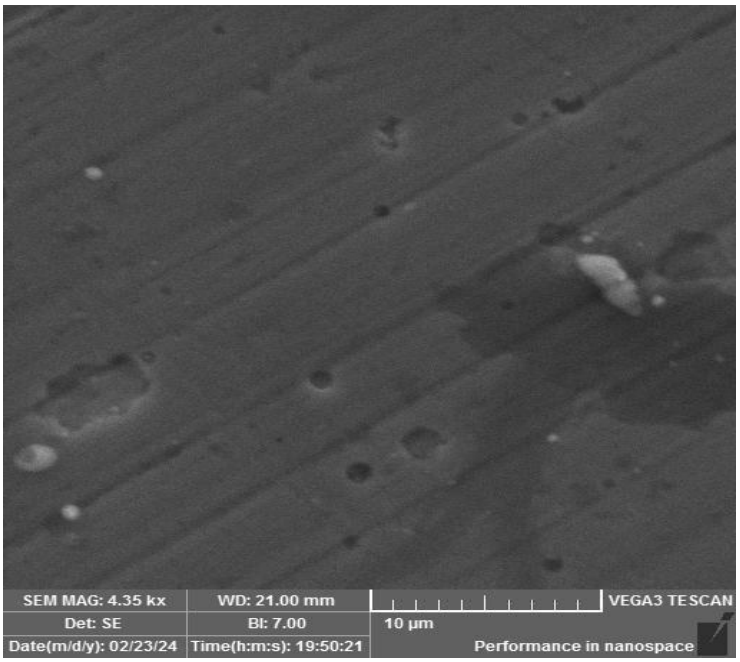

Figure 11 Uncoated SS316l SEM results

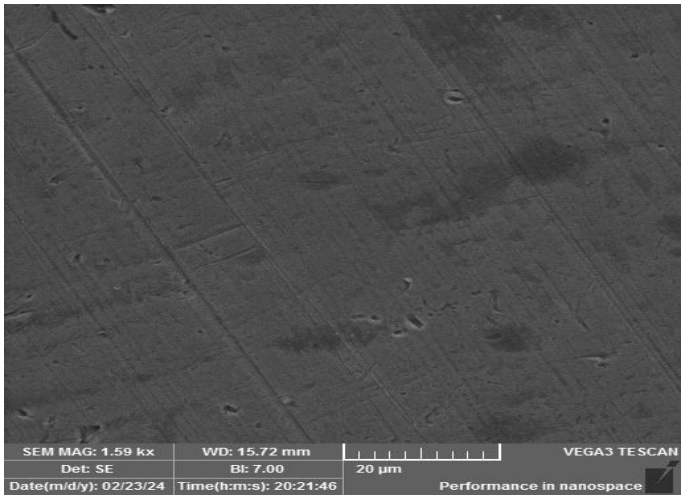

Figure 12: SEM results of thin TiO2 film deposited on SS-304L

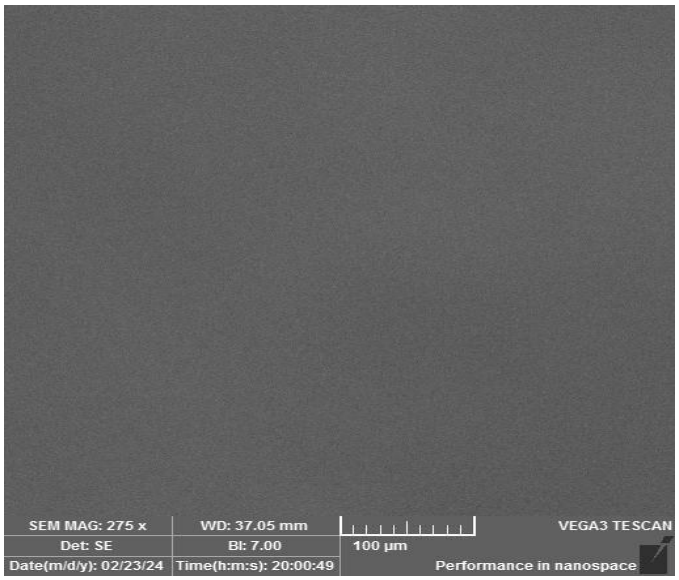

Figure 13: SEM and EDS results of thin TiO2 film deposited on SS-316L

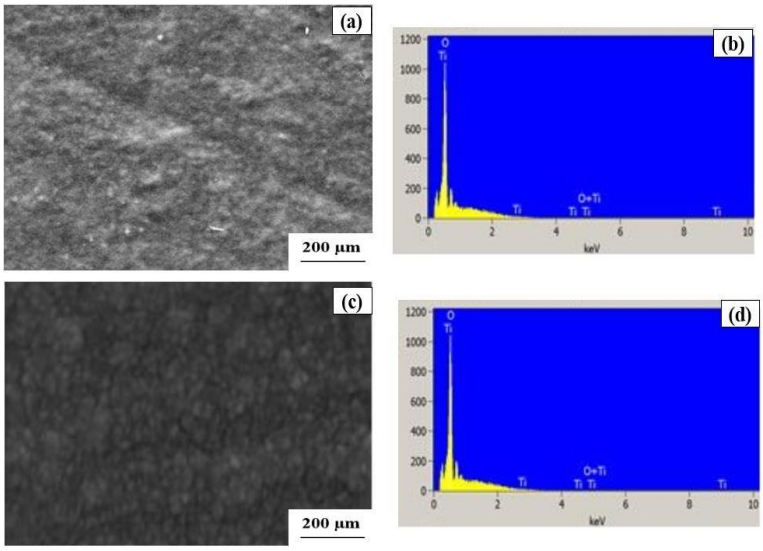

Figure 14: SEM and EDS results of thin TiO2 film deposited on SS-304L (a & b) and SS-316 L (c & d) respectively after corrosion.

EDS analysis confirmed the presence of titanium and oxygen, verifying successful coating. No significant impurities were observed. Grain boundary regions were more pronounced in SS-316L than SS-304L due to its molybdenum content, contributing to higher corrosion resistance. The microstructural refinement correlates with improved mechanical and corrosion properties [42].

3.4 Discussion on Observed Results

The electrochemical trends observed in the EIS response are strongly supported by the microstructural evidence obtained from SEM and EDS. The uncoated SS304L and SS316L surfaces Figures 10 and 11 exhibit polishing-induced grooves and localized surface heterogeneities, including micro-pits and dispersed contrast features. Such surface irregularities are well known to promote non-uniform passivation and facilitate preferential adsorption of chloride ions, thereby increasing the likelihood of localized breakdown and pitting in simulated physiological media. In practical terms, these microstructural discontinuities create micro-galvanic sites and local chemistry gradients under exposure, which is consistent with the smaller Nyquist semicircles and comparatively lower charge transfer resistance measured for the uncoated conditions. The uncoated SS304L, in particular, presents more pronounced micro-defect contrast and surface irregularity in the observed regions Figure 10, which provides a microstructural basis for its lowest corrosion resistance among the tested conditions and aligns with the ranking derived from the Nyquist response Figure 9.

In contrast, the TiO_2-coated specimens Figures 12 and 13 show a substantially more uniform surface appearance, indicating that the PVD process produced a continuous film that effectively masks or bridges the fine-scale surface features of the substrates. The coated SS304L surface Figure 12 displays a compact morphology with reduced prominence of discontinuities, while the coated SS316L surface Figure 13 appears highly homogeneous over a larger field of view, suggesting superior macroscopic uniformity and consistent coverage. This comparative uniformity provides a direct morphological explanation for the higher impedance response of coated samples, as a continuous ceramic layer reduces the effective electrochemically active area and suppresses direct charge transfer between the electrolyte and the underlying metal. Consequently, the measured increase in Rct from 2.5 to 8.3 $k\Omega \cdot cm^2$ for SS304L and from 4.1 to 12.7 $k\Omega \cdot cm^2$ for SS316L Table 1 is consistent with the formation of a dense barrier film that limits ionic transport and delays passive film breakdown. The superior corrosion performance of TiO_2-coated SS316L compared with TiO_2-coated SS304L is further supported by the apparent uniformity of the coated surface in Figure 13, which implies fewer defects or weak points that could serve as penetration pathways for chloride ions during prolonged exposure.

The post-corrosion SEM/EDS results Figure 14 provide additional evidence for coating stability and the mechanistic basis of corrosion protection in simulated physiological environments. The SEM micrographs in Figure 14(a) and 14(c) indicate that the coated surfaces maintain a coherent film-like morphology following electrochemical exposure, without signs of extensive delamination or catastrophic coating failure within the observed regions. Importantly, the associated EDS spectra in Figure 14(b) and 14(d) confirm the persistence of Ti and O as dominant surface constituents after corrosion testing, indicating that the TiO_2 layer remains present and chemically stable during exposure. This post-corrosion compositional

confirmation directly supports the claim that TiO_2 functions as a protective passive barrier and validates that the improved Nyquist semicircle diameter originates from coating-mediated interfacial resistance rather than short-term transient behavior. In the context of implant-related service conditions, retention of Ti–O surface chemistry after corrosion is a critical indicator of durable protection, as it suggests that the coating continues to isolate the metallic substrate and mitigate metal-ion release over time.

The mechanical property trends also remain consistent with the microstructural observations. The increase in Vickers hardness after coating Table 2 can be reasonably attributed to the presence of a hard ceramic TiO_2 film and to the improved surface integrity suggested by the coated micrographs Figures 12 and 13. A continuous and well-adherent thin film can increase resistance to near-surface deformation under indentation by constraining plastic flow and distributing the applied load more uniformly across the surface, thereby producing the observed 8–12% hardness increase. Meanwhile, the modest changes reported in compressive strength Table 3 are expected to be smaller than hardness changes because compressive strength is dominated by the bulk substrate; however, the post-deposition surface condition may still contribute indirectly by reducing the influence of surface micro-defects that can serve as crack initiation sites under compressive loading. In this respect, the smoother and more uniform coated surfaces observed in Figures 12–13, together with the absence of major coating failure after corrosion exposure Figure 14, support the conclusion that TiO_2 deposition improves surface-related mechanical response while preserving overall structural integrity.

Overall, the combined microstructural (SEM/EDS) and electrochemical evidence provides a coherent, mechanistic justification for the study's novelty: TiO_2 films deposited by PVD on SS304L and SS316L form stable and continuous barrier layers that persist after electrochemical exposure, resulting in a substantial increase in charge transfer resistance and a measurable enhancement in surface hardness without detrimental effects on bulk mechanical performance. This integrated correlation between morphology, chemistry, corrosion resistance, and mechanical response strengthens the claim that TiO_2-coated stainless steels offer improved long-term suitability for biomedical applications, particularly where chloride-rich physiological environments are expected.

4 Conclusion

This study focused and evaluated the effect of a thin titanium dioxide (TiO_2) coating deposited by physical vapor deposition (PVD) on SS304L and SS316L stainless-steel substrates to enhance their suitability for biomedical applications. The electrochemical results confirmed a substantial improvement in corrosion resistance for the coated specimens compared with the uncoated controls, evidenced by increased charge-transfer resistance and larger Nyquist semicircle diameters, with TiO_2-coated SS316L exhibiting the highest corrosion protection among all conditions. Mechanical testing further indicated that the coating process did not compromise structural integrity; instead, the coated samples showed an increase in surface hardness 12%, consistent with the presence of a hard ceramic surface layer, while compressive strength changed only modestly 7%, indicating preservation of bulk load-bearing behavior. Microstructural characterization supported these outcomes, as SEM observations revealed a continuous and homogeneous TiO_2 film without visible cracking or delamination, and EDS verified Ti and O enrichment on the coated surfaces, confirming successful coating formation and coverage. Overall, the combined electrochemical, mechanical, and

microstructural evidence demonstrates that PVD-deposited TiO_2 is an effective surface modification for improving the performance of stainless steels in simulated physiological environments, with TiO_2-coated SS316L emerging as the most promising candidate for long-term biomedical implant applications.

Data availability and material: All relevant data and material are visible in the manuscript.

Declarations: The authors declare that they have no known competing financial interests or personal relationships that could have appeared to influence the work reported in this paper.

Consent for publication: The manuscript is reviewed and approved by all authors.

Conflict of interest: The authors declare no competing interests.

5 References

[1] M. K. Abbass, S. A. Ajeel, and H. M. Wadullah, Biocompatibility, Bioactivity and Corrosion Resistance of Stainless Steel 316L Nanocoated with TiO2 and Al2O3 by Atomic Layer Deposition Method, J Phys Conf Ser, 1032(1) (2018).

[2] H. Wang, R. Zhang, Z. Yuan, X. Shu, E. Liu, and Z. Han, A comparative study of the corrosion performance of titanium (Ti), titanium nitride (TiN), titanium dioxide (TiO2) and nitrogen-doped titanium oxides (N–TiO2), as coatings for biomedical applications, Ceram Int, 41(9) 11844–11851.

[3] S. Nosheen, "Proliferation of Bovine Albumin Serum on Nano-Scale Titanium Nitride Coated Stainless Steel Substrates for Biomedical Applications," International Journal of Biomedical Materials Research, vol. 5, no. 5, p. 64, 2017, Doi: 10.11648/j.ijbmr.20170505.12.

[4] M. C. Mataya, E. R. Nilsson, E. L. Brown, and G. Krauss, "Hot working and recrystallization of as-cast 317L," Metall Mater Trans A Phys Metall Mater Sci, vol. 34, no. 12, pp. 3021–3041, 2003, Doi: 10.1007/s11661-003-0201-2.

[5] G. Singh, S. Singh, and S. Prakash, "Characterization and Corrosion Behavior of Plasma Sprayed Pure and Reinforced HA Coatings in Simulated Body Fluid," Journal of Minerals and Materials Characterization and Engineering, vol. 10, no. 09, pp. 765–775, 2011, Doi: 10.4236/jmmce.2011.109060.

[6] A. Ataollahi Oshkour, S. Pramanik, M. Mehrali, Y. H. Yau, F. Tarlochan, and N. A. Abu Osman, "Mechanical and physical behavior of newly developed functionally graded materials and composites of stainless steel 316L with calcium silicate and hydroxyapatite," J Mech Behav Biomed Mater, vol. 49, pp. 321–331, 2015, Doi:10.1016/j.jmbbm.2015.05.020.

[7] H. Bakhtiari-Zamani, E. Saebnoori, H. R. Bakhsheshi- Rad, and F. Berto, "Corrosion and Wear Behavior of TiO2/TiN Duplex Coatings on Titanium by Plasma Electrolytic Oxidation and Gas Nitriding," Materials, vol. 15, no. 23, pp. 1–17, 2022, Doi: 10.3390/ma15238300.

[8] D. Prando et al., "Corrosion of titanium: Part 2: Effects of surface treatments," J Appl Biomater Funct Mater, vol. 16, no. 1, pp. 3–13, 2018, Doi: 10.5301/jabfm.5000396.

[9] H. Shilkamy and A. Abdou, "Studies on Corrosion Behavior and Biomedical Applications of Titanium- based materials: A Comprehensive Review," Sohag Journal of Sciences, vol. 9, no. 3, pp. 297–307, 2024, Doi: 10.21608/sjsci.2024.243679.1137.

[10] S. Sun and X. Liu, "Experimental research on biomedical titanium coating corrosion effects," Chem Eng Trans, vol. 59, pp. 769–774, 2017, Doi: 10.3303/CET1759129.

[11] O. Kierat, A. Dudek, and L. Adamczyk, "The effect of the corrosion medium on silane coatings deposited on titanium grade 2 and titanium alloy ti13nb13zr," Materials, vol. 14, no. 21, 2021, Doi: 10.3390/ma14216350.

[12] S. Rudenja, P. Kulu, and V. Mikli, "Sergei RUDENJA," pp. 14–25, 1996.

[13] H. P. R. Corado, F. M. De Souza Soraes, D. M. Barbosa, A. M. Lima, and C. N. Elias, "Titanium Coated with Graphene and Niobium Pentoxide for Biomaterial Applications," Int J Biomater, vol. 2022, 2022, Doi: 10.1155/2022/2786101.

[14] D. Prando et al., "Corrosion of titanium: Part 1: Aggressive environments and main forms of degradation," J Appl Biomater Funct Mater, vol. 15, no. 4, pp. e291–e302, 2017, Doi: 10.5301/jabfm.5000387.

[15] H. A. Almashhadani and K. A. Saleh, “Corrosion protection of pure titanium implant by electrochemical deposition of hydroxyapatite post- anodizing,” IOP Conf Ser Mater Sci Eng, vol. 571, no. 1, 2019, Doi: 10.1088/1757 899X/571/1/012071.

[16] M. Ibrahim, J. B. Agboola, S. A. Abdulkareem, O. Adedipe, and J. O. Tijani, “Effects of elevated temperature on the corrosion resistance of silver– cobalt oxide–titanium dioxide (Ag/Co3O4/TiO2) nanocomposites coating on AISI 1020,” Sci Rep, vol. 11, no. 1, pp. 1–14, 2021, Doi: 10.1038/s41598-021- 90272-w.

[17] H. Kgomo et al., “Investigation of the corrosion behaviour of TiC/Ti6Al4V manufactured through laser additive manufacturing,” MATEC Web of Conferences, vol. 388, p. 08007, 2023, Doi: 10.1051/matecconf/202338808007.

[18] R. Malhotra, Y. Han, C. A. Nijhuis, N. Silikas, A. H. Castro Neto, and V. Rosa, “Graphene nanocoating provides superb long-lasting corrosion protection to titanium alloy,” Dental Materials, vol. 37, no. 10, pp. 1553–1560, 2021, Doi: 10.1016/j.dental.2021.08.004.

[19] M. Staszuk, D. Pakuła, Ł. Reimann, M. Musztyfaga- Staszuk, R. Socha, and T. Tański, “Investigation of Ti/Al2O3 + TiO2 and Ti + TiO2/Al2O3 + TiO2 hybrid coatings as protection of ultra-light Mg–(Li)–Al–RE alloys against corrosion,” Sci Rep, vol. 12, no. 1, pp. 1–18, 2022, Doi: 10.1038/s41598-022-23452-x.

[20] H. Acid, “Corrosion Resistance of Zircadyne,” Corrosion.

[21] E. S. M. Sherif, “A comparative study on the corrosion of pure titanium and titanium- 12%zirconium alloy after different exposure periods of time in sodium chloride solution,” AIP Adv, vol. 14, no. 3, 2024, Doi: 10.1063/5.0192701.

[22] S. W. Khan, G. Vinay, A. Kumar, P. Singh, and H. Singh, “Investigations on Corrosion Behaviour of Cold-Sprayed Titanium on SS316L Steel,” Journal of Thermal Spray and Engineering, vol. 4, pp. 100–105, 2024, Doi: 10.52687/2582-1474/404.

[23] H. KAMINAKA, M. ABE, S. KIMURA, K. MATSUMOTO, and H. KAMIO, “Characteristics and Applications of High Corrosion Resistant Titanium Alloys,” Nippon Steel & Sumitomo Metal Technical Report, vol. 104, no. 106, 2014, [Online]. Available: https://www.nipponsteel.com/en/tech/report/nssm c/pdf/106-07.pdf

[24] I. A. Polyakov, O. G. Lenivtseva, V. V. Samoylenko, M.

G. Colkovski, and I. S. Ivanchik, “Corrosion resistance of Ti-Ta-Zr coatings in the Boiling Acid Solutions,” IOP Conf Ser Mater Sci Eng, vol. 156, no. 1, pp. 4–8, 2016, Doi: 10.1088/1757-899X/156/1/012023.

[25] S. P. Collins et al., “No Title 済無No Title No Title No Title,” 2021.

[26] J. Vaughan and A. Alfantazi, “Corrosion of Titanium and Its Alloys in Sulfuric Acid in the Presence of Chlorides,” J Electrochem Soc, vol. 153, no. 1, p. B6, 2006, Doi: 10.1149/1.2126580.

[27] Matsuda Kiyoshi. "Akashi Hirotaka: Pioneer of Kyoto's Modernization - Exhibition Materials Catalog." (2022).

[28] M. T. Lin, C. H. Wan, and W. Wu, “Enhanced corrosion resistance of SS304 stainless steel and titanium coated with alternate layers of TiN and ZrN in a simulated O2-rich environment of a unitized regenerative fuel cell,” Int J Electrochem Sci, vol. 9, no. 12, pp. 7832–7845, 2014, Doi: 10.1016/s1452-3981(23)11009-1.

[29] F. Modiri and H. Savaloni, “A study of the corrosion of stainless steel 304L coated with a 190 nm-thick manganese layer and annealed with nitrogen flux in a 0.4-mole solution of H2SO4 at different temperatures,” Journal of Theoretical and Applied Physics, vol. 14, no. 1, pp. 21–35, 2020, Doi: 10.1007/s40094-019-00345-5.

[30] D. Alontseva et al., “Improving Corrosion and Wear Resistance of 316L Stainless Steel via In Situ Pure Ti and Ti6Al4V Coatings: Tribocorrosion and Electrochemical Analysis,” Materials, vol. 18, no. 3, pp. 1–16, 2025, Doi: 10.3390/ma18030553.

[31] R. R. Kumar et al., “Investigation of friction welding parameters of AISI 304L/Ti-6AL-4V joints,” Mater Res Express, vol. 9, no. 10, 2022, Doi: 10.1088/2053- 1591/ac9776.

[32] R. Ganesan, K. Rajeswari, “Corrosion Behavior of TiO_2 Coated Stainless Steel in Simulated Body Fluid,” Surface and Coatings Technology, vol. 203, no. 1, pp. 154–158, 2008.

[33] A. Balamurugan, S. Kannan, S. Rajeswari, Evaluation of TiO2 coatings obtained using the sol–gel technique on surgical grade type 316 L stainless steel in simulated body fluid, Mater. Lett. 59 (2005) 3138–3143.

[34] Wang, H., Zhang, R., Yuan, Z., Shu, X., Liu, E., & Han, Z. (2015). A comparative study of the corrosion performance of titanium (Ti), titanium nitride (TiN), titanium dioxide (TiO2) and nitrogen-doped titanium oxides (N–TiO2), as coatings for biomedical applications. Ceramics International, 41(9), 11844–11851.

[35] Zhang, L., et al. (2013). Improvement of corrosion resistance and biocompatibility of Ti alloys by TiO_2 coating. Materials Science and Engineering: C, 33, 1– 7.

[36] Song, Y., et al. (2004). Influence of surface oxide film on corrosion behavior of titanium alloy. Materials Science and Engineering: C, 24(6–8), 701–705.

[37] I.T. Hong, C.H. Koo, Antibacterial properties, corrosion resistance and mechanical properties of Cu-modified SUS 304 stainless steel, Mater. Sci. Eng. A 393 (2005) 213–222.

[38] Park, J.B., & Lakes, R.S. (2007). Biomaterials: An Introduction. Springer.

[39] Kuroda, S., et al. "Thermal Sprayed Hydroxyapatite Coatings for Biomedical Applications." Surface and Coatings Technology, vol. 89, 1997, pp. 38–43.

[40] G.J. Ma, G.Q. Lin, S.L. Gong, X. Liu, G. Sun, H.C. Wu, Mechanical and corrosive characteristics of Ta/TaN multilayer coatings, Vacuum 89 (2013) 244–248.

[41] P. Dearnley, “A Review of Metallic, Ceramic and Surface-Treated Metals Used for Hip and Knee Implants,” Journal of Materials Science: Materials in Medicine, vol. 7, pp. 381–401, 1996.

[42] A. Tekin, J.W. Martin, B.A. Senior, Grain boundary sensitization and desensitization during the ageing of 316 L(N) austenitic stainless steels, J. Mater. Sci. 26 (1991) 2458–2466.